



## Poly (ethylene glycol) prodrug for anthracyclines via N-Mannich base linker: Design, synthesis and biological evaluation

Yong-Jiang Zhao<sup>a,b</sup>, Wei Wei<sup>a,b</sup>, Zhi-Guo Su<sup>a</sup>, Guang-Hui Ma<sup>a,\*</sup>

<sup>a</sup> National Key Laboratory of Biochemical Engineering, Institute of Process Engineering, Chinese Academy of Sciences, P.O.Box353, Beijing 100190, China

<sup>b</sup> Graduate University of Chinese Academy of Sciences, Beijing 100049, China

### ARTICLE INFO

#### Article history:

Received 2 March 2009

Received in revised form 31 May 2009

Accepted 11 June 2009

Available online 18 June 2009

#### Keywords:

PEGylated prodrug

Anthracycline anticancer drug

N-Mannich base

### ABSTRACT

Poly (ethylene glycol)s (PEGs) are potential drug carriers for improving the therapeutic index of anticancer agents. In this work, a novel methodology for constructing PEG prodrug of anthracycline anticancer drugs was developed based on N-Mannich base of salicylamide and its 2-acyloxymethylated derivative. The resultant conjugates first subjected to in vitro hydrolysis testing, which revealed the release behavior of newly synthesized PEG prodrugs could be adjusted by the status of 2-hydroxy group of salicylamide. These PEG prodrugs also demonstrated superior cytotoxicity in antiproliferative assay. O-blocked doxorubicin prodrug with PEG20k as carrier was selected for further in vivo assessments and presented longer circulating life in pharmacokinetic experiment. This high molecular prodrug was also found to be more efficacious against S-180 xenografted tumor than equivalent amount of doxorubicin.

© 2009 Elsevier B.V. All rights reserved.

### 1. Introduction

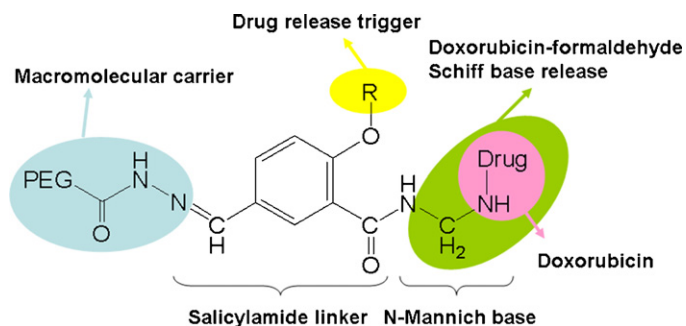
Since Prof. H. Ringsdorf proposed his famous model for rational design of polymer–drug conjugates (Ringsdorf, 1975), extensive efforts have been made to develop more efficient drug delivery system (DDS) based on this model (Kopecek et al., 2000; Li and Wallace, 2008; Hoste et al., 2004; Allen and Cullis, 2004; Greenwald et al., 2003). The advantages of rational designed polymer–drug conjugates include solubility of hydrophobic drugs; increased stability; passive and active targeting; and altered pharmacokinetics as well as controlled release of drugs (Hoste et al., 2004). For anticancer drug that exhibits narrow therapeutic index, DDS based on polymer–drug conjugates can be used potentially to minimize the adverse side effects and suppress cellular resistance (Haag and Kratz, 2006), and also target drug to tumor by enhanced permeability and retention (EPR) effect (Maeda et al., 2000) or other active methods (Chandna et al., 2007; Minko et al., 2004; Allen, 2002; Rihová et al., 2000). Over the last decade, nearly a dozen polymer–drug conjugates have entered clinical studies and early results have generally been promising (Li and Wallace (2008)).

In Ringsdorf's original model, a number of drug molecules are covalently bond to a macromolecule carrier through a degradable or reversible spacer. The kind of conjugates is often termed as polymeric prodrug or macromolecular prodrug (Hoste et al., 2004). The spacer in polymeric prodrug can incorporate a predetermined breaking point to ensure release of the drug at the site of inter-

est (D'Souza and Topp, 2004; Soyez et al., 1996). The design of drug–polymer conjugates initially focused on incorporating enzymatically cleavable bonds that allow the prodrug to be cleaved after cellular uptake (Subr et al., 1988; Kopecek et al., 2000; Veronese et al., 2005). Acid-sensitive (Rodrigues et al., 1999; Ulbrich et al., 2003; Ulbrich and Subr, 2004) and redox-sensitive linkers (Saito et al., 2003) have also been discussed for constructing macromolecular prodrugs. More versatile platforms employing 1,4- or 1,6-elimination (Greenwald et al., 1999) or trimethyl lock lactonization (Greenwald et al., 2000) have been introduced to PEG prodrug area by Greenwald. By using these prodrug strategies, alteration of macromolecular prodrug pharmacokinetics can be readily accomplished leading to greater drug efficacy. More recently, a cleavage mechanism involving triggering events that lead to a release cascade has been presented (Haba and Popkov, 2005; Shabat, 2006). The advantage of this approach is a high local drug concentration with a potential increase in efficacy. Since the linkage plays crucial factor in macromolecular prodrug, it is essential to develop new spacer or linker to widen the library of macromolecular prodrug strategies.

N-Mannich bases have been used successfully to obtain prodrugs of amine as well as amide-containing drugs (Bundgaard and Johansen, 1980). This structure with salicylamide as amide moiety has more unique hydrolysis process, a quick degradation triggered by the proton of 2-hydroxy group (Bundgaard, 1986; Fenich et al., 1997; Cogan et al., 2004). A number of targeting prodrugs for doxorubicin based on salicylamide N-Mannich base have been developed by Koch's group (Burkhart et al., 2004; Burke and Koch, 2004; Cogan and Koch, 2003). These prodrugs release doxorubicin-formaldehyde Schiff base, which subsequently serves

\* Corresponding author. Tel.: +86 10 82627072; fax: +86 10 82627072.  
E-mail address: [ghma@home.ipe.ac.cn](mailto:ghma@home.ipe.ac.cn) (G.-H. Ma).



Scheme 1. Structure of N-Mannich base PEG prodrugs.

to covalently modify genomic DNA, an event proposed to ultimately be more toxic than the mere intercalation of unmodified doxorubicin (Burkhart et al., 2004; Burke and Koch, 2004; Cogan and Koch, 2003).

In our exploit of new spacer for macromolecular prodrug, especially PEG prodrug, we considered that N-Mannich base with salicylamide as amide moiety might be an ideal structural platform from which to launch novel macromolecular prodrugs. Thus, the incorporation of PEG into the N-Mannich base system as macromolecular carrier results in a neutral and highly water-soluble polymeric prodrug capable of passive tumor targeting (Scheme 1). This PEG prodrug can be designed to attain predictable rates of hydrolysis by changing the status of 2-hydroxy of salicylamide. Moreover, the released drug–formaldehyde Schiff base changes the interaction mechanism of drug and genomic DNA, leading to superior antiproliferative response related to delivery parent drug alone. To fully exploit the N-Mannich base system for polymeric prodrugs, 5-formyl-salicylamide and its O-acyloxymethylated derivative were used as amide moiety to synthesize N-Mannich bases for two kinds of anthracycline anticancer drug: doxorubicin (DOX) and daunorubicin (DNR). Subsequently, PEG prodrugs were constructed by introducing PEG carrier through the formyl group. These PEG prodrugs were first subjected to evaluations of release behavior and in vitro antiproliferative activity. Afterwards, the pharmacokinetic property and antitumor activity of O-blocked mPEG20k prodrug were evaluated by in vivo experiments. In this way, we wanted to obtain a first insight into the mechanistic characteristics and biological activity of the newly synthesized PEG prodrugs.

## 2. Materials and methods

### 2.1. Materials

Methoxy PEG5k was obtained from Polysciences Inc. (Warrington, PA). Methoxy PEG20k was obtained from Nektar (Huntsville, AL). All PEG materials were dried azeotropically before use. Doxorubicin hydrochloride and daunorubicin hydrochloride came from Huafenglianbo Technology Company (Beijing, China). The cell supplies and agents were purchased from Gibco (Pailey, UK). All other reagents and solvents were obtained from Beijing Chemical Reagents Company (Beijing, China).

### 2.2. General methods

Reversed-phase HPLC was performed with LC-20AT and SPD-M20A system (SHIMADZU, Japan).

Inertsil ODS-3 (254 mm × 4.6 mm) C-18 reversed-phased column (SHIMADZU, Japan) was used for monitoring the synthesis of salicylamide and 2-acyloxymethylated salicylamide. Elution was carried out at a flow rate of 1 mL with a linear gradient of acetonitrile in water containing 0.05% (v/v) TFA from 10% to 70% over

40 min the effluent was monitored by recording the absorbance at 254 nm.

Vydac C<sub>4</sub> column (150 mm × 4.6 mm, particle size 5 μm) was used for monitoring the synthesis of PEG prodrug and the release behavior of PEG prodrugs. Elution was carried out at a flow rate of 0.5 mL with a linear gradient of acetonitrile in water containing 0.05% (v/v) TFA from 15% to 80% over 50 min. To characterize the different preparations, the effluent was monitored by recording the absorbance at 254 nm. 480 nm was used to measure the free drug content and the release behavior of PEG prodrugs.

GPC was carried out on Superdex75 (GE health, Sweden), mounted on an Agilent 1100 HPLC system, equipped with a degasser and a variable wavelength detector with UV monitoring at 254 nm. The column was eluted by 50 mM phosphate buffer, containing 0.1 M Na<sub>2</sub>SO<sub>4</sub>, pH 6.8, at a flow rate of 0.5 mL/min.

<sup>1</sup>H NMR and <sup>13</sup>C NMR spectra were recorded on an AVANCE Bruker 600 MHz spectrometer using DMSO-d<sub>6</sub> or CDCl<sub>3</sub> as solvents separately in 5 mm NMR tubes. In all the spectra TMS was used as the internal reference.

Mass spectra were carried out on a LCQ Deca XP Thermo Finnigan (San Jose, CA) ion trap MS equipped with an electrospray ionization source. The mass spectrometer was operated in positive ion mode.

### 2.3. Synthesis of mPEG candidates

#### 2.3.1. Synthesis of mPEG5k-ONH<sub>2</sub>

**2.3.1.1. Synthesis of mPEG5k-Br.** Methoxy PEG5k (5 g, 1 mmol) was dissolved in 50 mL toluene and the solvent was refluxed to azeotropically remove water for 6 h. The solution was evaporated to dryness under vacuum. The residue was dissolved in 20 mL dry CH<sub>2</sub>Cl<sub>2</sub>. Triphenylphosphine (390 mg, 1.5 mmol) and CBr<sub>4</sub> (150 μL, 1.5 mmol) were added under N<sub>2</sub> and the resulting solution was stirred under room temperature for 24 h. The solution was then dried over vacuum. The residue was dissolved in water and filtered off. The aqueous phase was then extracted with three portions of CH<sub>2</sub>Cl<sub>2</sub> of 45 mL. The combined extracts were dried over Na<sub>2</sub>SO<sub>4</sub> and evaporated under vacuum to about 10 mL. The solution was precipitated with diethyl ether and dried under vacuum to obtain the product as a white powder (4.8 g, 96% yield). <sup>1</sup>H NMR (DMSO-d<sub>6</sub>): 3.24 (CH<sub>3</sub>O-, 3H), 3.51 (PEG main chain). The disappearance of triplet at 4.56 ppm (proton of hydroxy group of mPEG) gave evidence that the conversion of mPEG-Br was quantitative.

**2.3.1.2. Synthesis of N-mPEG-phthalimide (mPEG5k-NHP).** Methoxy PEG5k-Br (5 g, 1 mmol) was dissolved in dry DMF, N-hydroxyphthalimide (200 mg, 1.2 mmol) and triethylamine (180 μL, 1.2 mmol) was added under N<sub>2</sub>. The suspension was stirred vigorously under 110 °C for 12 h. After DMF was removed under vacuum, the resulting mixture was dissolved in brine water and filtered off. The aqueous phase was then extracted with three portions of 45 mL CH<sub>2</sub>Cl<sub>2</sub>. The combined extracts were dried over Na<sub>2</sub>SO<sub>4</sub> and evaporated under vacuum to about 10 mL. The solution was precipitated with diethyl ether and dried under vacuum to obtain the product as a white powder (4.9 g, 98% yield). <sup>1</sup>H NMR (DMSO-d<sub>6</sub>): 3.24 (CH<sub>3</sub>O-, 3H), 3.51 (PEG main chain), 7.75 (m, 2H), 7.82 (m, 2H).

**2.3.1.3. Converting mPEG5k-NHP to mPEG5k-ONH<sub>2</sub>.** Cleavage of the phthalimide moiety was achieved by adding hydrazine hydrate (80 μL, 3 mmol) to a solution of the PEG5k-NHP product (5 g, 1 mmol) dissolved in CH<sub>2</sub>Cl<sub>2</sub> (10 mL). The solution was stirred rapidly for 0.5 h, during which a white precipitate was observed. After filtration, the solution was precipitated with diethyl ether and dried under vacuum to obtain the product as a white powder (4.5 g, 90% yield). <sup>1</sup>H NMR (DMSO-d<sub>6</sub>): 3.24 (CH<sub>3</sub>O-, 3H), 3.51 (PEG main chain).

### 2.3.2. Synthesis of mPEG-CONHNH<sub>2</sub>

**2.3.2.1. Synthesis of mPEG succinimide ester (mPEG-SCM).** Methoxy PEG5kCOOH was synthesized according to our previous report (Li et al., 2005). Methoxy PEG5kCOOH (5 g, 1 mmol) was dissolved in 50 mL toluene and the solvent was refluxed to azeotropically remove water for 6 h. The solution was evaporated to dryness under vacuum. The residue was dissolved in 20 mL dry CH<sub>2</sub>Cl<sub>2</sub>. N-hydroxy-succinimide (150 mg, 1.5 mmol) and dicyclohexyl carbodiimide (300 mg, 1.5 mmol) were added under N<sub>2</sub>. The solution was stirred for 12 h at room temperature, during which a white precipitate was observed. After filtration, the solution was concentrated to about 10 mL under vacuum. The solution was then precipitated with diethyl ether and dried under vacuum to obtain the product as a white powder (4.9 g, 98% yield). <sup>1</sup>H NMR (DMSO-d<sub>6</sub>): 3.24 (CH<sub>3</sub>O-, 3H), 3.51 (PEG main chain), 3.98 (2H, CH<sub>2</sub>COOH), 2.84 (4H, CH<sub>2</sub> in succinimide).

**2.3.2.2. Synthesis of mPEG5k hydrazide.** Methoxy PEG5k-SCM (5 g, 1 mmol) was dissolved in CH<sub>2</sub>Cl<sub>2</sub> (10 mL). Hydrazine hydrate (80 μL, 3 mmol) was added under N<sub>2</sub>. The solution was stirred rapidly for 0.5 h, during which a white precipitate was observed. After filtration, the solution was then precipitated with diethyl ether and dried under vacuum to obtain the product as a white powder (4.5 g, 90% yield). <sup>1</sup>H NMR (DMSO-d<sub>6</sub>): 3.24 (CH<sub>3</sub>O-, 3H), 3.51 (PEG main chain), 3.98 (2H, CH<sub>2</sub>CONHNH<sub>2</sub>).

### 2.4. Synthesis of O-free and O-blocked 5-formyl-salicylamide

#### 2.4.1. Synthesis of 5-formyl-salicylamide

Labetalol hydrochloride (2 g, 5.6 mmol) was dissolved in 500 mL water. The pH value of the solution was adjusted to 10 by saturated NaHCO<sub>3</sub> solution. Then, sodium periodate (1.2 g, 5.6 mmol) in 50 mL of H<sub>2</sub>O was added by drop-wise manner over 30 min the solution was stirred for another 30 min, and acidified with 3.0 mL of concentrated HCl. The resulting suspension was stored for 12 h at 4 °C to form white precipitation, and then filtered. The collected solid was crystallized from 80 mL of boiling water and allowed to sit for 12 h at 4 °C. Vacuum filtration gave 700 mg of product as white to golden power (71% yield). <sup>1</sup>H NMR (DMSO-d<sub>6</sub>): 7.06 (1H, d, J = 8 Hz, 3), 7.95 (1H, dd, J = 8, 2 Hz, 4), 8.13 (1H, bs, NH), 8.44 (1H, d, J = 2 Hz, 6), 8.65 (1H, bs, NH), 9.98 (1H, s, 5CHO); <sup>13</sup>C NMR (DMSO-d<sub>6</sub>): 191, 171, 166, 134, 132, 128, 118, 115.

#### 2.4.2. Synthesis of chloromethylacetate

Anhydrous ZnCl<sub>2</sub> (150 mg) was added to thionyl chloride (50 mL) and the mixture was heated to reflux for 6 h. After the removal of thionyl chloride under vacuum, paraformaldehyde (1.5 g, 50 mmol) was added at 4 °C in an ice bath. Acetyl chloride (6 mL, 75 mmol) was added to this mixture in a drop-wise manner over 1 h. After addition was complete, the ice bath was removed and the mixture was heated to reflux at 55 °C for 24 h. At this time, vacuum distillation at 40 °C and 10 mmHg gave 2.45 g (40% yield) of chloromethylacetate as a clear, colorless oil. <sup>1</sup>H NMR (CDCl<sub>3</sub>): 2.16 (3H, s, AcO), 5.68 (2H, s, OCH<sub>2</sub>Cl).

#### 2.4.3. Synthesis of 2-acetoxymethoxy-5-formyl-benzamide

A mixture of 5-formyl-salicylamide (1.6 g, 10 mmol) and potassium carbonate (3.2 g, 10 mmol) was stirred for 30 min at room temperature in 50 mL of acetone. In a separated flask, chloromethylacetate (2 g, 10 mmol) and potassium iodide (3.5 g, 10 mmol) were stirred in 30 mL of acetone at room temperature. The two reactions were then combined and refluxed for 4 h. The reaction was stopped by cooling to room temperature and filtering through a glass frit. The collected liquid was rotary evaporated and the residue was dissolved in 100 mL of ethyl acetate. After being washed with saturated brine, the organic layer was collected and dried

over anhydrous magnesium sulfate. Concentration by rotary evaporation followed by recrystallization from ethyl acetate/hexanes yielded 412 mg (25% yield) of the desired 2-acetoxymethoxy-5-formyl-benzamide. <sup>1</sup>H NMR (DMSO-d<sub>6</sub>): 2.16 (3H, s, AcO), 5.96 (2H, s, OCH<sub>2</sub>O), 6.20 (1H, bs, NH), 7.30 (1H, d, J = 8 Hz, 3), 7.44 (1H, bs, NH), 8.02 (1H, dd, J = 8, 2 Hz, 4), 8.71 (1H, d, J = 2 Hz, 6), 10.00 (1H, s, 5CHO).

### 2.5. General method for N-Mannich reaction

The following procedure was used to synthesize the O-free DOX N-Mannich base as an example.

20 μL of a 37% formalin solution was added to a stirring solution of 20 mg 5-formyl-salicylamide in 2.0 mL DMF. The reaction was stirred in a screw top vial for 15 min at 55 °C, during which time 20 mg of doxorubicin hydrochloride was added to form a red suspension which was stirred at 55 °C. After 15 min, a clear red solution had formed and the reaction was removed from the heat. Transfer of the solution to 30 mL cool ethyl ether and centrifugation to afford red power. The red power was readily dissolved in 20 mL of methanol containing 30% water (1% TFA). After 10 min at room temperature, the methanol was removed by rotary evaporation and the resulting aqueous solution was diluted to 100 mL with saturated brine, transferred to a separatory funnel. Extraction into 50 mL of chloroform followed by rotary evaporation at 30 °C gave a red film. The product was then dissolved in 3 mL of chloroform and introduced to a silica gel flash column (1 cm × 15 cm) which had been packed in 100% chloroform. Contaminants were eluted with 100% chloroform followed by 97.5% chloroform/2.5% methanol. The desired product was then eluted with 95% chloroform/5% methanol and isolated by rotary evaporation at 30 °C. The solvent free product was dissolved in 1 mL of chloroform and precipitated by the addition of 5 mL of hexanes. Centrifugation, followed by decanting of the supernatant and drying under vacuum yielded the desired product as a red solid. The product was characterized by <sup>1</sup>H NMR and MS spectrum as report above.

#### 2.5.1. O-free DOX N-Mannich base

<sup>1</sup>H NMR (DMSO-d<sub>6</sub>): 13.93/13.26 (2H, bs, d6/d11OH), 9.84 (1H, s, CHO), 8.54 (1H, d, J = 2 Hz, s6), 8.02 (1H, d, J = 8 Hz, s4), 7.89 (1H, d, J = 8 Hz, d1), 7.78 (1H, t, J = 8 Hz, d2), 7.37 (1H, d, J = 8 Hz, d3), 7.14 (1H, d, J = 8 Hz, s3), 5.48 (1H, s, d1'), 5.16 (1H, s, d7), 4.78 (1H, bs, d9OH), 4.72 (d14,s, 2H), 4.34 (2H, dd, J = 13, 6 Hz, NCH<sub>2</sub>N), 4.07 (3H, s, OCH<sub>3</sub>), 3.72 (1H, s, d4'), 3.14 (1H, d, J = 17 Hz, d10), 2.93 (1H, d, J = 17 Hz, d10), 2.35 (1H, d, J = 8 Hz, d8), 2.06 (1H, dd, J = 16.4 Hz, d8), 1.70–1.87 (2H, m, d2'), 1.38 (3H, d, J = 6 Hz, d5'CH<sub>3</sub>). [MH<sup>+</sup>] 721.0 (calculated for 721.2).

#### 2.5.2. O-blocked DOX N-Mannich base

<sup>1</sup>H NMR (DMSO-d<sub>6</sub>): 13.89/13.12 (2H, bs, d6/d11OH), 9.89 (1H, s, CHO), 8.54 (1H, d, J = 2 Hz, s6), 8.02 (1H, d, J = 8 Hz, s4), 7.91 (1H, dd, J = 8, 2 Hz, d1), 7.78 (1H, t, J = 8 Hz, d2), 7.37 (1H, d, J = 8 Hz, d3), 7.14 (1H, d, J = 8 Hz, s3), 5.83 (1H, d, J = 8 Hz, OCH<sub>2</sub>O), 5.68 (1H, d, J = 8 Hz, OCH<sub>2</sub>O), 5.48 (1H, s, d1'), 5.16 (1H, s, d7), 4.74 (d14,s, 2H), 4.36 (2H, dd, J = 12, 5 Hz, NCH<sub>2</sub>N), 4.07 (3H, s, OCH<sub>3</sub>), 3.73 (1H, s, d4'), 3.14 (1H, d, J = 17 Hz, d10), 2.93 (1H, d, J = 17 Hz, d10), 2.35 (1H, d, J = 8 Hz, d8), 2.06 (1H, dd, J = 16.4 Hz, d8), 2.04 (3H, s, AcO), 1.63–1.84 (2H, m, d2'), 1.39 (3H, d, J = 6 Hz, d5'CH<sub>3</sub>). [MH<sup>+</sup>] 793.0 (calculated for 793.2).

#### 2.5.3. O-free DNR N-Mannich base

<sup>1</sup>H NMR (CDCl<sub>3</sub>): 13.93/13.25 (2H, bs, d6/d11OH), 9.91 (1H, s, s5CHO), 8.54 (1H, d, J = 2 Hz, s6), 8.02 (1H, d, J = 8 Hz, s4), 7.89 (1H, dd, J = 8, 2 Hz, d1), 7.78 (1H, t, J = 8 Hz, d2), 7.37 (1H, d, J = 8 Hz, d3), 7.14 (1H, d, J = 8 Hz, s3), 5.53 (1H, s, d1'), 5.27 (1H, s, d7), 4.68 (1H, bs, d9OH), 4.34 (2H, dd, J = 12, 5 Hz, NCH<sub>2</sub>N), 4.07 (1H, s, OCH<sub>3</sub>), 3.72

(1H, s, d4'), 3.14 (1H, d,  $J=17$  Hz, d10), 2.93 (1H, d,  $J=17$  Hz, d10), 2.37 (3H, s, d14), 2.35 (1H, d,  $J=8$  Hz, d8), 2.06 (1H, dd,  $J=16.4$  Hz, d8), 1.69–1.83 (2H, m, d2'), 1.38 (3H, d,  $J=6$  Hz, d5'CH<sub>3</sub>). [MH<sup>+</sup>] 703.0 (calculated for 703.2).

#### 2.5.4. O-blocked DNR N-Mannich base

<sup>1</sup>H NMR (CDCl<sub>3</sub>): 13.94/13.17 (2H, bs, d6/d11OH), 9.89 (1H, s, CHO), 8.54 (1H, d,  $J=2$  Hz, s6), 8.02 (1H, d,  $J=8$  Hz, s4), 7.94 (1H, d,  $J=8$  Hz, d1), 7.78 (1H, t,  $J=8$  Hz, d2), 7.37 (1H, d,  $J=8$  Hz, d3), 7.14 (1H, d,  $J=8$  Hz, s3), 5.83 (1H, d,  $J=8$  Hz, OCH<sub>2</sub>O), 5.68 (1H, d,  $J=8$  Hz, OCH<sub>2</sub>O), 5.48 (1H, s, d1'), 5.16 (1H, s, d7), 4.68 (1H, bs, d9OH), 4.36 (2H, dd,  $J=12, 5$  Hz, NCH<sub>2</sub>N), 4.07 (3H, s, OCH<sub>3</sub>), 3.72 (1H, s, d4'), 3.14 (1H, d,  $J=17$  Hz, d10), 2.93 (1H, d,  $J=17$  Hz, d10), 2.37 (3H, s, d14), 2.35 (1H, d,  $J=8$  Hz, d8), 2.06 (1H, dd,  $J=16.4$  Hz, d8), 2.02 (3H, s, AcO), 1.70–1.87 (2H, m, d2'), 1.38 (3H, d,  $J=6$  Hz, d5'CH<sub>3</sub>). [MH<sup>+</sup>] 775.0 (calculated for 775.3).

The yield of N-Mannich reaction was about 50–60%, varied in different batch.

#### 2.6. General method for synthesis of PEG prodrug

Methoxy PEG5k hydrazide (50 mg, 0.01 mmol) or mPEG20k hydrazide (200 mg, 0.01 mmol) were dissolved in 10 mL of ethanol (95%). N-Mannich base of anthracycline anticancer drugs (9 mg, 0.15 mmol) and 50  $\mu$ L trifluoroacetic acid was added. The reaction mixture was stirred vigorously for 6 h. After evaporation of the ethanol, the residue was purified by GPC using a Superdex75 column. The PEG conjugate fractions were then extracted with CH<sub>2</sub>Cl<sub>2</sub>, and the extracts were dried over Na<sub>2</sub>SO<sub>4</sub> and evaporated under vacuum to about 10 mL. Cold ethyl ether was added, and the resulting precipitate was collected by vacuum filtration and dried under vacuum to obtain the product as pink powder (about 80% yielding, varied in different batches). Total drug content was measured by UV/vis absorbance at 480 nm using parent drug as reference. Free drug content was calculated by peak ratio of free drug and PEG prodrug at 480 nm.

#### 2.7. Evaluation of drug release

For hydrolysis in buffer, PEG derivatives were dissolved in 0.1 M pH 7.4 PBS buffer in 5 mg/mL. For hydrolysis in plasma, the derivatives were dissolved in distilled water at a concentration of 20 mg/100  $\mu$ L and 900  $\mu$ L of rat plasma was added to this solution. The mixture was vortexed for 5 min and divided into glass vials with 100  $\mu$ L of aliquot/vial. The solutions were incubated at 37 °C for various periods of time. A mixture of methanol–acetonitrile (1:1, v/v, 400  $\mu$ L) was added to a vial at the proper interval and the mixture was vortexed for 1 min, followed by centrifugation at 4000  $\times$  g and filtration through 0.45  $\mu$ m filter membrane. An aliquot of 20  $\mu$ L of the filtrate was injected into the HPLC. On the basis of the peak area, the amounts of native compound and PEG derivatives were estimated, and the half-time of each compound in different media was calculated using linear regression analysis from the disappearance of PEG derivative.

#### 2.8. Cell line and cell culture

The leukemia cell line K562 and cervical cancer cell line HeLa were gifts from Peking University. K562 cell was cultured in RPMI1640 standard medium supplemented with 10% (v/v) fetal calf serum in humidified atmosphere of 95% air and 5% CO<sub>2</sub> at 37 °C. HeLa cell was cultured in DMEM standard medium supplemented with 10% (v/v) fetal calf serum in humidified atmosphere of 95% air and 5% CO<sub>2</sub> at 37 °C.

#### 2.9. Cytotoxicity of DNR against K562 cells and DOX against HeLa cells

In vitro cytotoxicity was determined by MTT assay. K562 or HeLa cells were aliquoted to 96-well plates at a density of  $2.0 \times 10^5$  cells/mL. Subsequently, serial dilutions of native and PEGylated drugs were added. After incubated for 24 h, the cells were treated with MTT for 4 h. The formed formazan crystals were then dissolved in isopropanol and absorbance was measured at 570 nm on a Bio-Rad model 550 microplate reader. The cell viability of native drug or PEG prodrug was expressed as percentages of the control and IC<sub>50</sub> values were determined by sigmoidal dose–response fitting of cell viability vs. doxorubicin equivalent concentration.

#### 2.10. Nuclear staining with Hoechst 33342

K562 cells were aliquoted to 6-well plates at a density of  $2.0 \times 10^5$  cells/mL, and incubated with native DNR, O-free and O-blocked PEG5k prodrug (0.4  $\mu$ mol/L) for 6 h. Cells were washed with PBS and incubated with 4  $\mu$ g/mL of Hoechst 33342, a DNA-binding fluorescent dye, for 30 min at 37 °C. The morphological characteristics of apoptotic cells were identified under a fluorescent microscope Eclipse80i (Nikon, Japan) with excitation at 540 nm. Cells with fragmented and/or condensed nuclei were classified as apoptotic cells.

#### 2.11. Doxorubicin levels in plasma and pharmacokinetic parameters

Drugs were injected via a lateral tail vein into 18–20 g normal male ICR mice at the dose of 1.5 mg/kg. With a certain time interval after i.v. administration of drug, 200  $\mu$ L of blood was collected from a capillary in the retroorbital plexus and directly mixed with 50  $\mu$ L of sodium citrate (4% solution). Plasma was then immediately centrifuged at 4000  $\times$  g at 4 °C for 20 min. Plasma doxorubicin concentrations were measured using a microplate fluorescence reader Infinite™ 200 (TECAN, Switzerland) with fluorescence detection. The excitation wavelength used was 480 nm and the emission wavelength was 560 nm. The pharmacokinetic parameters of doxorubicin and its PEG prodrug were calculated. Elimination half-lives ( $t_{1/2}$ ) were determined by linear regression analysis after log transforming concentrations. From the concentration profiles of doxorubicin in plasma, we calculated volumes of distribution ( $V_d$ ) and clearances (CL) (Lee et al., 2007).

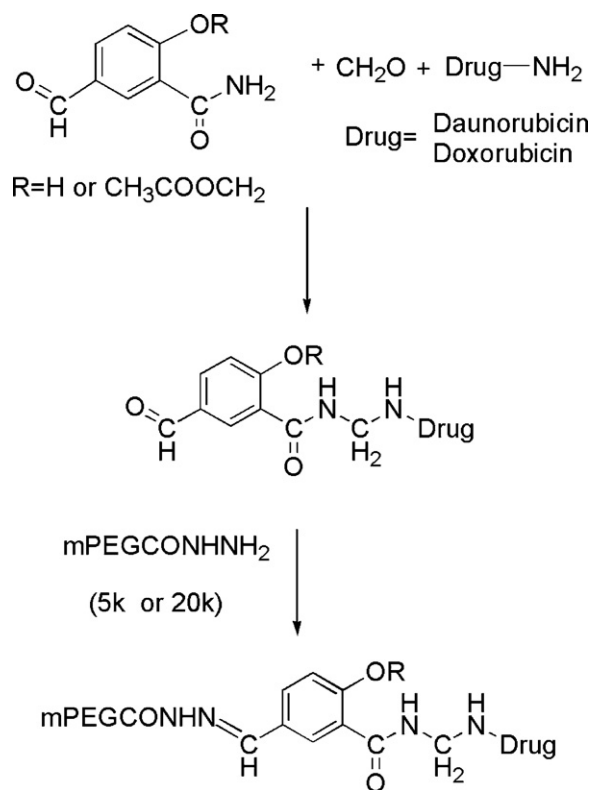
#### 2.12. Inhibition effect on the growth of S-180 xenografted tumor

Tumor bearing mice were prepared by inoculating a suspension of  $4 \times 10^6$  cells into the shaved right dorsa of 7-week-old male ICR mice (20–22 g) on day 0. On day 1, the mice were randomized into control and treatment groups ( $n=5$ ). They were injected via a lateral tail vein with saline, free DOX or O-blocked PEG20k-DOX. The precise dose and schedule is shown in Section 3. The experiment was terminated after 2 weeks and the animals were humanely killed. The weight of tumor tissue was measured and the inhibition rates of growth of S-180 xenografted tumors were calculated according to the formula: inhibition rate (%) =  $(1 - \text{mean weight (treatment)}/\text{mean weight (control)}) \times 100$ .

### 3. Results and discussions

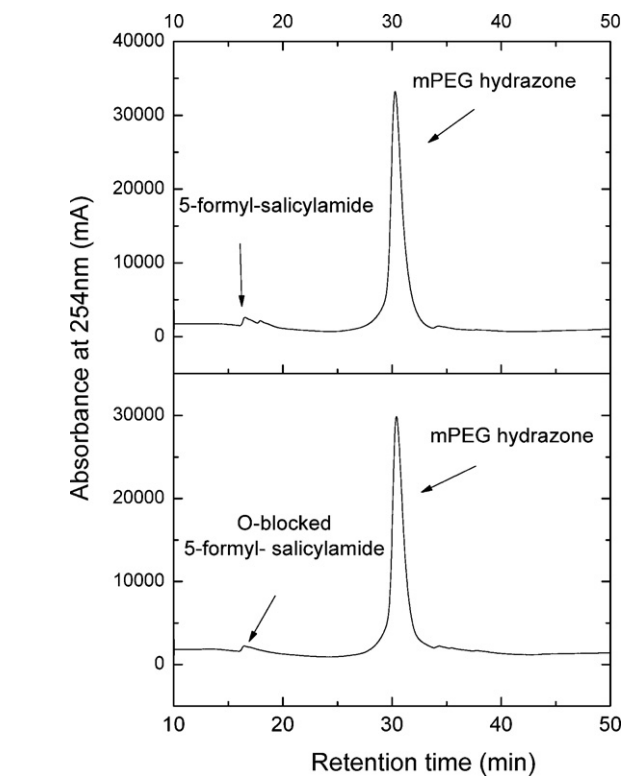
#### 3.1. Chemistry of PEG N-Mannich base prodrug

Two-step synthesis strategy was decided to construct N-Mannich base PEG prodrugs (Scheme 2). First, anthracycline

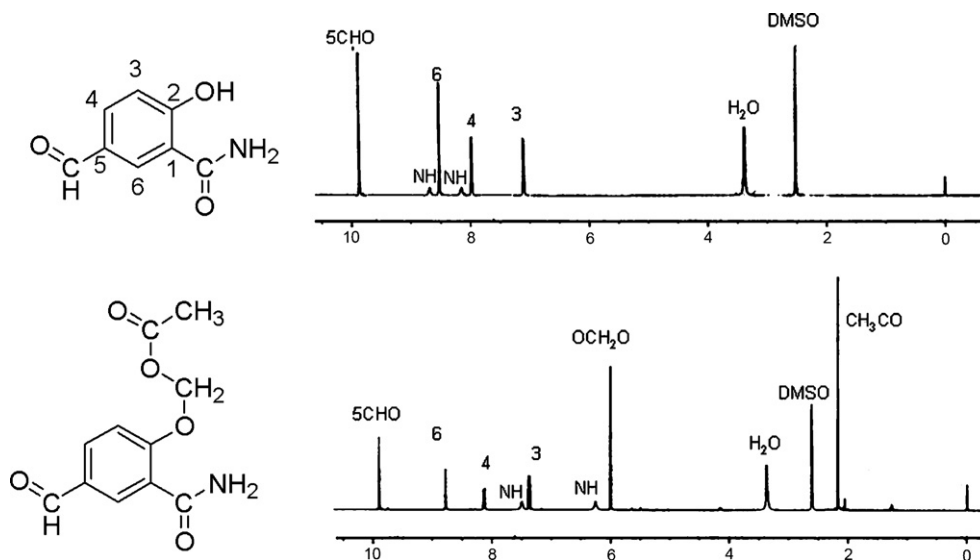


anticancer drug was linked to 5-formyl salicylamide or its O-blocked derivative by N-Mannich reaction. Then, PEG carrier with different molecular weight was attached through the formyl group. 5-formyl-salicylamide was prepared from oxidation of Labetalol hydrochloride by sodium periodate (Salomies et al., 1989). O-blocked 5-formyl-salicylamide was prepared by O-acyloxymethylation of 5-formyl-salicylamide with chloromethylacetate (Bundgaard, 1986; Reich, 2000). The structure of 5-formyl-salicylamide and its O-blocked derivative were confirmed by  $^1\text{H}$  NMR (Fig. 1).

Three mPEG derivatives, mPEG amine (Zalipsky et al., 1983), mPEG aminoxy (Schlick et al., 2005) and mPEG hydrazide



(Martinez et al., 1997) were synthesized as candidates for macromolecular carrier. In our preliminary experiments, the reactivity of mPEG amine to formyl group was weak, whereas mPEG aminoxy and mPEG hydrazide could readily react with 5-formyl-salicylamide. In fact, the chemoselective reaction between PEG hydrazide or aminoxy and ketone (aldehyde) has been extensively used to modify protein in a site-specific manner (Kochendoerfer, 2005). In this study, mPEG hydrazide was used as macromolecular carrier for further exploit. When PEG hydrazide reacted with equivalent molar of 5-formyl-salicylamide only trace amounts of small molecule remained free (Fig. 2), indicating the high efficacy of hydrazone formation under acidic catalysis.



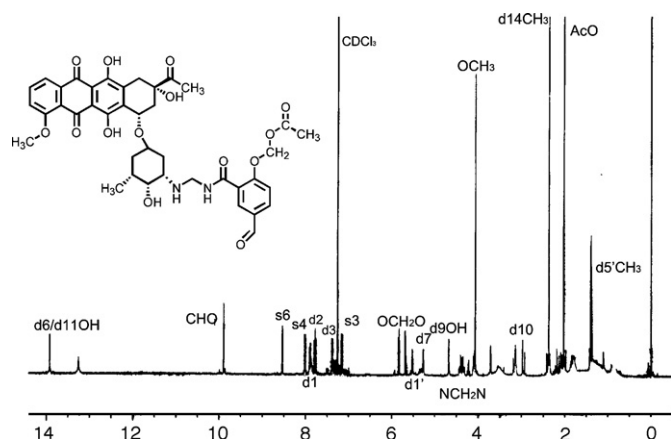


Fig. 3.  $^1\text{H}$  NMR spectrum of O-blocked N-Mannich Base of DNR.

According to Scheme 2, N-Mannich reaction was first performed to link anthracycline anticancer drug to salicylamide or its O-blocked derivative. The N-Mannich reaction between anthracycline anticancer drug and salicylamide was carried out in warm DMF and the desired product was isolated by flash silica column with moderate yield. The resulting O-free or O-blocked N-Mannich base was confirmed by Mass spectrum and  $^1\text{H}$  NMR spectrum. The  $^1\text{H}$  NMR spectra of O-blocked N-Mannich base of daunorubicin was exemplified in Fig. 3. The conjugation of N-Mannich bases to PEG hydrazide was accomplished in 95% ethanol under acidic catalysis. Excess equivalents of N-Mannich base were used to achieve complete conjugation of the PEG hydrazide. After conjugation, free N-Mannich base was eliminated using GPC chromatography. The resulting PEG prodrug was confirmed by single peak of HPLC at 254 nm (Fig. 4). The total and free drug content of all conjugates was shown in Table 1. The total drug content of the conjugate was calculated by UV/vis absorption at 480 nm using respective parent compound as reference and free drug content was calculated by peak ratio of free drug to PEG prodrug on HPLC graph (480 nm).

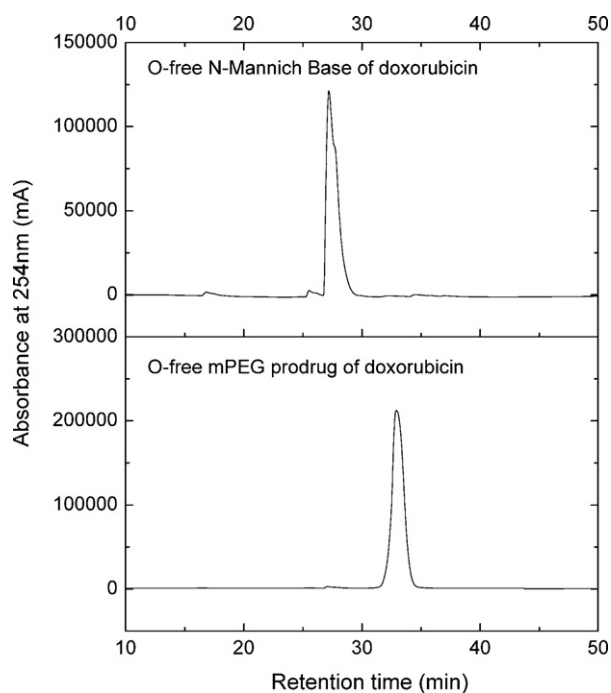


Fig. 4. HPLC of O-free DOX N-Mannich base and its PEG5k prodrug.

Table 1  
Composition of Various PEG prodrugs.

Compound	Structure	Total drug content (wt.%)	Free drug content
1	O-free PEG5k-DOX	7.1	1.7%
2	O-blocked PEG5k-DOX	7.2	0.9%
3	O-free PEG20k-DOX	2.5	2.1%
4	O-blocked PEG20k-DOX	2.6	1.5%
5	O-free PEG5k-DNR	7.2	1.2%
6	O-blocked PEG5k-DNR	7.3	0.8%

The total DNR or DOX content of the conjugate was calculated by UV absorption at 480 nm using respective parent compound as reference and free drug content was calculated by peak ratio of free anthracyclines and PEG prodrug at 480 nm. The amount of unconjugated free PEG remaining in samples was not evaluated.

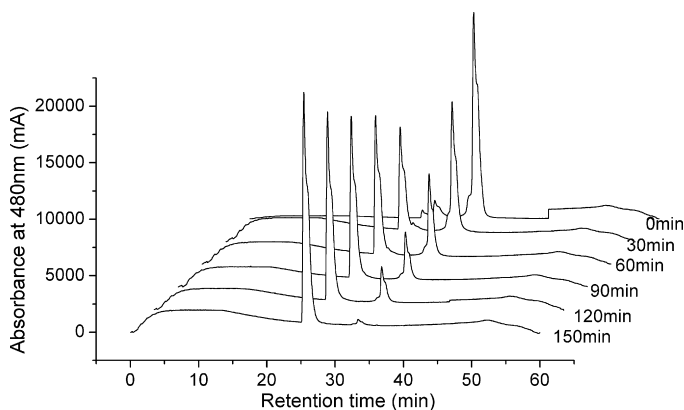


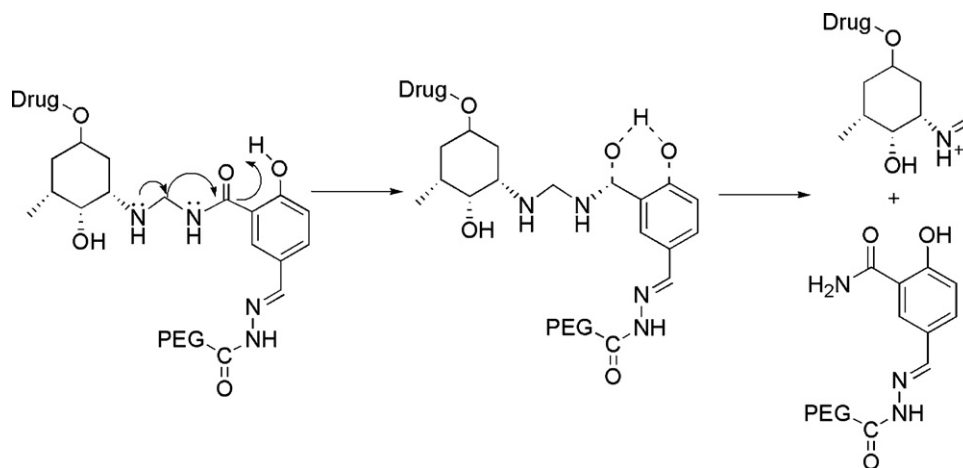
Fig. 5. Release profile of doxorubicin from O-free mPEG5k prodrug in PBS buffer (pH 7.4).

### 3.2. Release kinetics of PEG prodrug

The release kinetic of macromolecular prodrug has significant influence on both its safety and efficacy in vivo. Therefore, the hydrolysis behavior of newly synthesized PEG prodrugs was first evaluated in PBS buffer or rat plasma by HPLC at 480 nm. The loss of PEG prodrug was seen to be a clean process which generated quantitative amounts of parent drug (Fig. 5). The release half-lives of PEG doxorubicin prodrugs (Compounds 1–4) in both PBS buffer and plasma were calculated by linear regression and listed in Table 2. PEG prodrug based on 2-OH free salicylamide quickly released parent drug with half-time less than 1 h both in buffer and in plasma. These results revealed the hydrolysis of O-free prodrug required no external activation factors. According to the report of Bundgaard (1986), an intramolecular event triggered by 2-hydroxy of salicylamide accounted for the quick degradation of the prodrugs (Scheme 3). PEG prodrug prepared from protected salicylamide was found to be more stable than O-free PEG prodrug with half-life of more than 12 h at physiological temperature and pH. When O-blocked prodrug was subjected to plasma, the acyloxymethylated group was quickly cleaved by serum esterase. After the retrieval of 2-hydroxy group, the proton of this group triggered the intramolecular event to catalyze the release of parent drug. These results were consistent with the report of Bundgaard (1986).

Table 2  
Half lives of PEG prodrugs in PBS buffer and plasma.

Compound	Structure	$t_{1/2}$ (min) buffer pH 7.4	$t_{1/2}$ (min) rat plasma
1	PEG5k-DOX	45	52
2	O-blocked PEG5k-DOX	>720	144
3	PEG20k-DOX	53	45
4	O-blocked PEG20k-DOX	>720	168



**Scheme 3.** Partial hydrolysis of N-Mannich base PEG prodrug of doxorubicin.

and Koch's group (Cogan et al., 2004), indicating the hydrolysis of PEG prodrugs can be controlled by the status of 2-hydroxy group. The O-blocked conception of N-Mannich base allowed for the formation of PEG prodrug platform with tunable drug release behavior. With hydrolysis half-life of 2–3 h, the O-acyloxymethylated prodrug developed in this study may be promising for further exploit (Greenwald et al., 2000).

After endocytosis, the PEG prodrug is subjected to acidic environment of endosome or lysosome (Ulbrich and Subr, 2004). The acidic liable of hydrazone linkage between PEG carrier and N-Mannich base may result in complex release behavior at low pH environment: the cleavage of hydrazone linkage and N-Mannich base linkage occur simultaneously. Nevertheless, chromatogrammes of O-free prodrug cleavage at pH 5 (Fig. 6) showed clean release process similar to that at pH 7.4 (Fig. 5). To fully understand the degradation behavior of PEG prodrug at acidic condition, the cleavage rate of hydrazone linkage and N-Mannich base was evaluated, respectively. At pH 5 and 37 °C, hydrolysis of hydrazone between PEG and 5-formyl-salicylamide showed half life more than 12 h, while the degradation of O-free N-Mannich base with half-life about 1 h was much faster. Therefore, the predominant behavior of PEG prodrug at acidic condition still is the cleavage of N-Mannich base.

### 3.3. In vitro tumor cell inhibition

The in vitro cytotoxicity of doxorubicin prodrug was evaluated by MTT assay using HeLa (cervical cancer) cell line. The half maximal inhibitory concentration ( $IC_{50}$  value) of the test drugs was

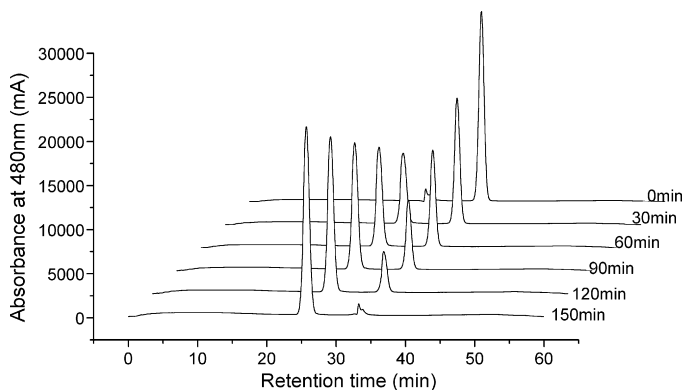


**Fig. 6.** Release profile of doxorubicin from O-free mPEG5k prodrug in PBS buffer (pH 5).

**Table 3**

$IC_{50}$  values of PEG prodrugs and their parent drugs.

Compound	Structure	Cell line	$IC_{50}$ ( $\mu\text{mol/L}$ )
DOX	–	HeLa	12.057
1	O-free PEG5k-DOX	HeLa	11.212
2	O-blocked PEG5k-DOX	HeLa	14.552
DNR	–	K562	0.421
5	O-free PEG5k-DNR	K562	0.207
6	O-blocked PEG5k-DNR	K562	0.411

calculated by sigmoidal dose–response fitting of cell viability vs. doxorubicin equivalent concentration (Table 3). The two prodrugs show comparable cytotoxicity in vitro as doxorubicin and the O-free prodrug even has a lower  $IC_{50}$  value (11.212  $\mu\text{mol/L}$ ) than parent drug (12.057  $\mu\text{mol/L}$ ). There are two reasons accounting for the antiproliferic response of DOX prodrugs. The first reason is the release manner of N-Mannich base prodrugs. It is common experience that rapid release behavior in plasma often leads to low  $IC_{50}$  value in vitro. The second reason is the partial hydrolysis of PEG N-Mannich base prodrug (Scheme 3), which generates the active metabolite, N-(hydroxymethyl)-doxorubicin, leading to remarkably efficient covalent modification of DNA (Cogan et al., 2004). Fig. 7 also demonstrated PEG carrier (the conjugate of PEG hydrazide and 5-formyl-salicylamide) had only slightly inhibition

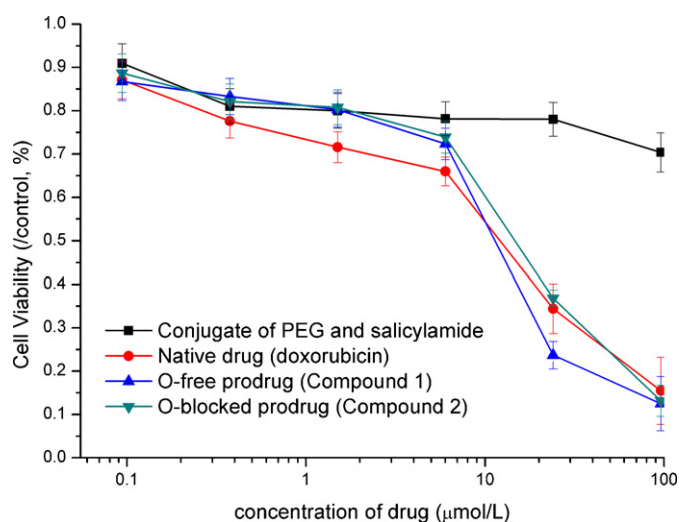


**Fig. 7.** Cytotoxicity of cells incubated with serial dilutions of DOX or its prodrugs.

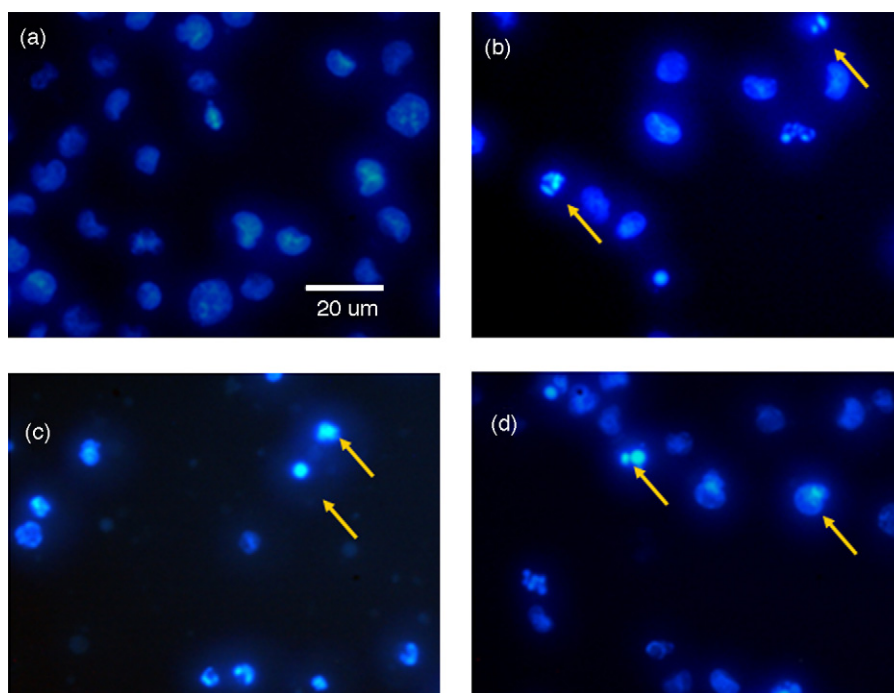


**Fig. 8.** Nuclear morphology change of K562 induced by DNR and DNR prodrugs (a: control, b: incubated with DNR, c: incubated with Compound 5 and d: incubated with Compound 6).

to tumor cells. It appeared that the anticancer agents are responsible for in vitro cytotoxicity observed. With passive accumulation in tumor by EPR effect, the superior cytotoxicity may widen the therapeutic index of PEG prodrugs. However, in vivo test is necessary to further verify the in vitro cytotoxicity result of prodrugs.

To extend the scope of our new PEG prodrug methodology, DNR prodrugs were also constructed in this study. The in vitro cytotoxicity of DNR prodrugs was investigated against K562 cell line (myelogenous leukaemia). The  $IC_{50}$  value of DNR prodrugs was also at the same level of parent compound. Hoechst stain demonstrated changes in nuclear morphology of K562 cell induced by DNR and DNR prodrugs. Compared to the typical round nuclei of control cell, cells incubated with prodrugs and parent drug displayed condensed and fragmented nuclei (Fig. 8), indicating different stages of apoptosis (Doonan and Cotter, 2008).

### 3.4. Drug level in plasma

An important factor leading to improved efficacy of polymer conjugates is the increased plasma residence time. Thus it is necessary to evaluate whether PEG prodrug based on N-Mannich base could circulate in the body for a longer time than parent compound. O-blocked mPEG20k prodrug (Compound 4) was selected for pharmacokinetic study because O-free prodrug released parent drug in a quick manner. After injecting doxorubicin and O-blocked mPEG20k prodrug, doxorubicin concentrations in blood were evaluated and all pharmacokinetic parameters were calculated. As shown in Fig. 9, the plasma level of doxorubicin in the doxorubicin group reached a nadir within 10 min whereas the plasma levels of PEG prodrug group declined more slowly. Actually, the plasma level of O-blocked mPEG20k prodrug was maintained for more than 2 h. The pharmacokinetic parameters ( $V_d$ , CL and  $t_{1/2}$ ) were listed in Table 4. The clearance value (6.62 mL/min) of PEG prodrug was remarkably lower than the 120 mL/min of doxorubicin, implying that the prodrug was eliminated much more slowly from the body than doxorubicin. These results suggested PEG prodrug based on N-Mannich base of O-blocked salicylamide could provide prolonged serum

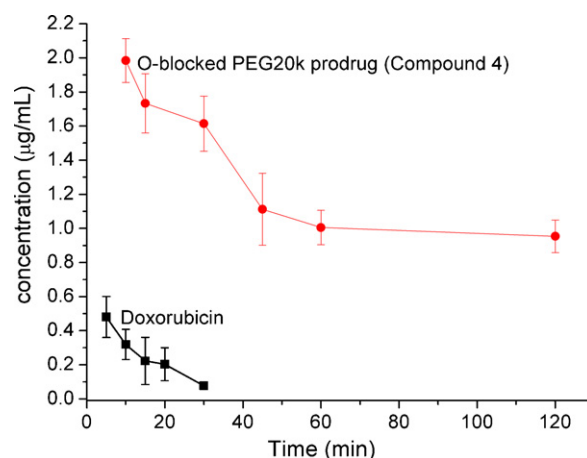


**Fig. 9.** Concentration profiles of doxorubicin in plasma after i.v. injection of DOX and O-blocked mPEG20k prodrug.

level of doxorubicin. In general, slow elimination promotes better access of drugs to remote targets. Further study was warranted with mPEG20k O-blocked prodrug to determine its antitumor activity in vivo.

### 3.5. Antitumor activity of PEG conjugate

The therapeutic potential of O-blocked mPEG20k prodrug (Compound 4) was further studied using solid tumor model. We compared the activity of DOX and O-blocked PEG20k-DOX at

**Table 4**  
Pharmacokinetic parameters of DOX and O-blocked PEG20k-DOX.

Compound	Structure	$k$ ( $\text{min}^{-1}$ )	$t_{1/2}$ (min)	$V_d$ (L/kg)	CL (mL/min)
DOX	–	0.1219	5.68	1.04	120
4	O-blocked PEG20k-DOX	0.0138	50.21	0.48	6.62



**Table 5**  
Treatment of Mice Bearing S-180 Tumor with DOX and O-blocked PEG20k-DOX.

Treatment <sup>a</sup>	Dose <sup>b</sup> (mg/kg DOX-equiv)	Tumor weight(g) <sup>c</sup> (mean ± SD)	Inhibition rate <sup>d</sup>	Average weight (% initial weight)
Saline	–	1.90 ± 0.45	0%	138%
DOX	3	1.06 ± 0.23 <sup>NS</sup>	44.07%	108%
O-blocked PEG20k-DOX (Compound 4)	3	0.77 ± 0.09* (*)	59.81%	125%
O-blocked PEG20k-DOX (Compound 4)	5	0.69 ± 0.12* (*)	65.14%	116%

<sup>a</sup> Group size is  $n = 5$ .

<sup>b</sup> Three i.v. injection on days 1, 3 and 6.

<sup>c</sup> Statistical significance was calculated using a Student's  $t$  test for small sample sizes. \* $p < 0.05$  and NS = not significant. Statistical significant between the PEG-conjugates vs. doxorubicin was shown in the bracket.

<sup>d</sup> Inhibition rate =  $(1 - \text{mean weight (treatment)/mean weight (control)}) \times 100$ .

3 mg/kg DOX-equiv dose on S-180 xenografted tumors, which has been used to evaluate doxorubicin contained micelles (Greish et al., 2004). The PEGylated DOX showed approximately 59% tumor growth inhibition compared to untreated control, while native DOX suppressed tumor growth only by 44% (Table 5). We concluded the enhanced antitumor activity resulted from combined effect of superior antiproliferative activity, increased circulating time and EPR-mediated targeting. Treatment with 5 mg/kg dose of prodrug caused slightly higher tumor inhibition compared to 3 mg/kg dose of prodrug. Therefore, more experiment was needed to determine the optimum dosage of this macromolecular prodrug. Additionally, it is noteworthy throughout this experiment that the PEG-DOX conjugate was less toxic as evidenced by its less effect on animal weight loss (Table 5).

#### 4. Conclusions

PEG prodrugs of anthracyclines were designed and synthesized using O-free or blocked salicylamide N-Mannich base as reversible linkage. In vitro hydrolysis assay demonstrated that the O-blocked conception of salicylamide N-Mannich base allowed for the formation of PEG prodrugs with controlled release behavior. All conjugates regardless of 2-hydroxy status showed comparable cytotoxicity as parent drugs in antiproliferative assay. Pharmacokinetic experiment revealed O-blocked mPEG20k prodrug provided longer circulating life than parent drug. This high molecular prodrug was also found to be more efficacious against S-180 xenografted tumor than equivalent amount of doxorubicin. Thus, we conclude that N-Mannich base of salicylamide indeed offers a very practical approach for constructing PEG prodrugs.

#### Acknowledgements

This work was financially supported by the National High-Tech R&D Program of China (863 Program) (2007AA021604) and the Chinese Academy of Sciences (KJCX2-YW-201-1). We also acknowledged the financial support from National Basic Research Program of China (2009CB930300).

#### Appendix A. Supplementary data

Supplementary data associated with this article can be found, in the online version, at doi: 10.1016/j.ijpharm.2009.06.013.

#### References

Allen, T.M., 2002. Ligand-targeted therapeutics in anticancer therapy. *Nat. Rev. Cancer* 2, 750–763.  
 Allen, T.M., Cullis, P.R., 2004. Drug delivery systems: entering the mainstream. *Science* 303, 1818–1822.  
 Bundgaard, H., 1986. Prodrugs as drug delivery systems. 43. O-acyloxymethyl salicylamide N-Mannich bases as double prodrug forms for amines. *Int. J. Pharm.* 29, 19–28.

Bundgaard, H., Johansen, M., 1980. Prodrugs as drug delivery systems IV: N-Mannich bases as potential novel prodrugs for amides, ureides, amines, and other NH-acidic compounds. *J. Pharm. Sci.* 69, 44–46.  
 Burke, P.J., Koch, T.H., 2004. Design, synthesis, and biological evaluation of doxorubicin–formaldehyde conjugates targeted to breast cancer cells. *J. Med. Chem.* 47, 1193–1206.  
 Burkhart, D.J., Kalet, B.T., Coleman, M.P., Post, G.C., Koch, T.H., 2004. Doxorubicin–formaldehyde conjugates targeting  $\alpha_v\beta_3$  integrin. *Mol. Cancer Ther.* 3, 1593–1604.  
 Chandna, P., Saad, M., Wang, Y., Ber, E., Khandare, J., Vetcher, A.A., Soldatenkov, V.A., Minko, T., 2007. Targeted proapoptotic anticancer drug delivery system. *Mol. Pharm.* 4, 668–678.  
 Cogan, P.S., Fowler, C.R., Post, G.C., Koch, T.H., 2004. Doxsaliform: a novel N-Mannich base prodrug of a doxorubicin formaldehyde conjugate. *Lett. Drug Des. Discov.* 1, 247–255.  
 Cogan, P.S., Koch, T.H., 2003. Rational design and synthesis of androgen receptor-targeted nonsteroidal anti-androgen ligands for the tumor-specific delivery of a doxorubicin–formaldehyde conjugate. *J. Med. Chem.* 46, 5258–5270.  
 Doonan, F., Cotter, T.G., 2008. Morphological assessment of apoptosis. *Methods* 44, 200–204.  
 D'Souza, A.J.M., Topp, E.M., 2004. Release from polymeric prodrugs: linkages and their degradation. *J. Pharm. Sci.* 93, 1962–1979.  
 Fenich, D.J., Taatjes, D.J., Koch, T.H., 1997. Doxoform and daunoform: anthracycline formaldehyde conjugates toxic to resistant tumor cells. *J. Med. Chem.* 40, 2452–2461.  
 Greenwald, R.B., Choe, Y.H., Conover, C.D., Shum, K., Wu, D., Royzen, M., 2000. Drug delivery systems based on trimethyl lock lactonization: poly(ethylene glycol) prodrugs of amino-containing compounds. *J. Med. Chem.* 43, 475–487.  
 Greenwald, R.B., Choe, Y.H., Mcguire, J., Conover, C.D., 2003. Effective drug delivery by PEGylated drug conjugates. *Adv. Drug Deliv. Rev.* 55, 217–250.  
 Greenwald, R.B., Pendri, A., Conover, C.D., Zhao, H., Choe, Y.H., Martinez, A., Shum, K., Guan, S., 1999. Drug delivery systems employing 1,4- or 1,6-elimination: poly(ethylene glycol) prodrugs of amine-containing compounds. *J. Med. Chem.* 42, 3657–3667.  
 Greish, K., Sawa, T., Fang, J., Akaike, T., Maeda, H., 2004. SMA-doxorubicin, a new polymeric micellar drug for effective targeting to solid tumours. *J. Control. Rel.* 97, 219–230.  
 Haag, R., Kratz, F., 2006. Polymer therapeutics: concepts and applications. *Angew. Chem. Int. Ed.* 45, 1198–1215.  
 Haba, K., Popkov, M., Shamis, M., Lerner, R.A., Barbas C.F.III, Shabat, D., 2005. Single-triggered trimeric prodrugs. *Angew. Chem. Int. Ed.* 44, 716–720.  
 Salomies, H., Luukkainen, L., Knuutila, R., 1989. Oxidation of  $\beta$ -blocking agents. VII. Periodate oxidation of labetalol. *J. Pharm. Biomed. Anal.* 7, 1447–1451.  
 Hoste, K., DE Winne, K., Schacht, E., 2004. Polymeric prodrugs. *Int. J. Pharm.* 277, 119–131.  
 Kochendoerfer, G.G., 2005. Site-specific polymer modification of therapeutic proteins. *Curr. Opin. Chem. Biol.* 9, 555–560.  
 Kopecek, J., Kopeckov, P., Minko, T., Lu, Z.-R., 2000. HPMA copolymer–anticancer drug conjugates: design, activity, and mechanism of action. *Eur. J. Pharm. Biopharm.* 50, 61–81.  
 Lee, G.Y., Park, K., Kim, S.Y., Byun, Y., 2007. MMPs-specific PEGylated peptide–DOX conjugate micelles that can contain free doxorubicin. *Eur. J. Pharm. Biopharm.* 67, 646–654.  
 Li, X.Q., Meng, F.T., Ma, G.H., Su, Z.G., 2005. A simple and efficient method for synthesis of carboxymethylated polyethylene glycol. *J. Chem. Res.* 5, 280–281.  
 Li, C., Wallace, S., 2008. Polymer–drug conjugates: recent development in clinical oncology. *Adv. Drug Deliv. Rev.* 60, 886–898.  
 Maeda, H., Wu, J., Sawa, T., Matsumura, Y., Hori, K., 2000. Tumor vascular permeability and the EPR effect in macromolecular therapeutics: a review. *J. Control. Rel.* 65, 271–284.  
 Martinez, A., Pendri, A., Xia, J., Greenwald, R.B., 1997. Branched poly(ethylene glycol) linkers. *Macromol. Chem. Phys.* 198, 2489–2498.  
 Minko, T., Dharap, S.S., Pakunlu, R.I., Wang, Y., 2004. Molecular targeting of drug delivery systems to cancer. *Curr. Drug Targets* 5, 389–406.  
 Reich, S.H., 2000. Substituted benzamide Inhibitors of human rhinovirus 3C Protease: structure-based design, synthesis, and biological evaluation. *J. Med. Chem.* 43, 1670–1683.

- Ríhová, B., Jelinkova, M., Strohalm, J., Subr, V., Plocov, D., Hovorka, O., Novak, M., Plundrov, D., Germano, Y., Ulbrich, K., 2000. Polymeric drugs based on conjugates of synthetic and natural macromolecules. II. Anti-cancer activity of antibody or (Fab')<sub>2</sub>-targeted conjugates and combined therapy with immunomodulators. *J. Control. Rel.* 64, 241–261.
- Ringsdorf, H., 1975. Structure and properties of pharmacologically active polymers. *J. Polym. Sci. Polym. Symp.* 51, 135–153.
- Rodrigues, P.C.A., Beyer, U., Schumacher, P., Roth, T., Fiebig, H.H., 1999. Acid-sensitive polyethylene glycol conjugates of doxorubicin: preparation, in vitro efficacy and intracellular distribution. *Bioorg. Med. Chem.* 7, 2517–2524.
- Saito, G., Swanson, J.A., LEE, K.-D., 2003. Drug delivery strategy utilizing conjugation via reversible disulfide linkages: role and site of cellular reducing activities. *Adv. Drug Deliv. Rev.* 55, 199–215.
- Schlick, T.L., Ding, Z., Kovacs, E.W., Francis, M.B., 2005. Dual-surface modification of the tobacco mosaic virus. *J. Am. Chem. Soc.* 127, 3718–3723.
- Shabat, D., 2006. Self-immolative dendrimers as novel drug delivery platforms. *J. Polym. Sci. A: Polym. Chem.* 44, 1569–1578.
- Soyez, H., Schacht, E., Vanderkerken, S., 1996. The crucial role of spacer groups in macromolecular prodrug design. *Adv. Drug Deliv. Rev.* 21, 81–106.
- Subr, V., Kopecek, J., Pohl, J., Baudys, M., Kostka, V., 1988. Cleavage of oligopeptide side-chains in N-(2-hydroxypropyl)meth-acrylamide copolymers by mixtures of lysosomal enzymes. *J. Control. Rel.* 8, 133–140.
- Ulbrich, K., Etrych, T., Chytil, P., 2003. HPMA copolymers with pH-controlled release of doxorubicin: in vitro cytotoxicity and in vivo antitumor activity. *J. Control. Rel.* 87, 33–47.
- Ulbrich, K., Subr, V., 2004. Polymeric anticancer drugs with pH-controlled activation. *Adv. Drug Deliv. Rev.* 56, 1023–1050.
- Veronese, F.M., Schlavon, O., Pasut, G., Mendichi, R., Andersson, L., Tsirk, A., Ford, J., Wu, G., Kneller, S., Davies, J., Duncan, R., 2005. PEG–doxorubicin conjugates: influence of polymer structure on drug release, in vitro cytotoxicity, biodistribution, and antitumor activity. *Bioconjugate Chem.* 16, 775–784.
- Zalipsky, S., Gilon, C., Zilkha, A., 1983. Attachment of drugs to polyethylene glycols. *Eur. Polym. J.* 19, 1177–1183.